# An integrated computational model for the optimisation of monolith catalytic converters

Clarkson, R. , Benjamin, S.F. , Jasper, T. and Girgls, N.

931071

# An Integrated Computational Model for the Optimisation of Monolith Catalytic Converters

R. J. Clarkson, S. F. Benjamin, T. S. Jasper, and N. S. Girgis
Coventry Univ.

## ABSTRACT

With the increasingly widespread use of catalytic converters for meeting exhaust emission regulations, considerable attention is currently being directed towards improving their performance. Experimental analysis is costly and time consuming. A desirable alternative would be a computational model based on established numerical techniques. To this end a transient three-dimensional model has been developed using a commercial CFD code. It simulates the fluid dynamics, chemical kinetics and heat and mass transfer that takes place in catalysts and their associated assembly. As a result the model can be used to predict important performance parameters such as conversion efficiency, incurred pressure drop and the thermal environment.

## INTRODUCTION

Over the last 20 years computational fluid dynamics (CFD) has grown from being an esoteric mathematical discipline into an engineering design and development tool. A major contributory factor to this has been the development, since 1980, of a number of commercially available general purpose CFD codes. These have opened up the field to relatively non-mathematical engineers. Additionally, improvements in numerical techniques and algorithms have meant that increasingly realistic engineering problems can be tackled. It has also been recognised within many industries that accurate computational modelling can be significantly less costly and time consuming than experimental analysis. The automotive industry is no exception, CFD having found several areas of application. One such area is the design of exhaust systems and catalytic converters.

Since the introduction of catalysts in the USA during the early 1970's considerable research has been carried out into the parameters that affect their performance. Early workers [1,2,3] soon established that the flow distribution across the monolith face significantly affects conversion efficiency and longevity. Much of the most recent work carried out using CFD has been aimed at studying the effect catalyst system geometry has on flow distribution [4]. Ways of improving the flow distribution have also been sought [5]. Although such studies are able to predict flow distributions, they are only dealing with fluid dynamics, consequently they are unable to directly measure the effect catalyst geometry has on conversion efficiency. One way around this problem is to model the conversion processes separately, any required velocity profiles being taken from CFD simulations [5,6] or experimental data [13,14,15]. There are however drawbacks to modelling the thermodynamics and chemistry of a catalyst as a separate entity. It is difficult to model the feedback effects the conversion processes have on flow distribution and until recently a purpose built computer code has been required. Developing such codes is time consuming, costly and needs a degree of expertise in numerical techniques.

Another area of interest for automotive designers is reducing the elevated exhaust back pressures that catalysts cause. Purely fluid dynamics models can only be used to predict some of the catalyst pressure drop phenomena. They are unable to predict the effects that variations in gas density and viscosity, caused by the conversion processes, have on pressure drop.

An obvious solution to these problems would be to utilise a commercial CFD code to model the fluid dynamics, heat and mass transfer and chemical kinetics that occur in catalysts and their associated duct work as an integrated system. This paper outlines a method developed to utilise the numerical algorithms of the commercial CFD code PHOENICS to build such a model.

## EXISTING CATALYST MODELS

Since the mid 1970's a number of computational models of single catalyst channels have been developed [7,8,9,10,11,12]. These models are of limited use for studying the behaviour of a complete catalyst in that they assume adiabatic channel conditions and a uniform monolith velocity profile. More recent studies, notably by Flytzani-Stephanopoulos et al. [13], Zygourakis [14], Chen et al. [15] and Will and Bennett [6], have modelled catalyst monoliths as a whole, with heat transfer between adjacent channels and non-uniform velocity profiles. All these models however suffer from one or more of the drawbacks discussed above. They include, to some extent, a purpose built numerical algorithm for solving the chemical kinetics and heat and mass transfer. Also, with the exception of Will and Bennett, there is no way of modelling the effects the conversion processes have on the velocity profile. Will and Bennett provided a feedback link to the velocity profile, which was predicted by a catalyst fluid dynamics model, by coupling the monolith pressure drop term with the fluid properties predicted by the conversion process model. However their model suffers from the limitation of only being able to simulate steady state conditions. Thus it cannot be used to study catalyst transient conditions, such as light-off.

Although it is conceivable that a catalyst could be modelled in its entirety, with each individual channel having its thermofluid dynamic processes simulated, such a model would be prohibitively large. It has been estimated that a computational grid in excess of $10^7$ cells would be required which would be problematic for most organisations. To avoid using extremely large grids two approaches have been developed, the equivalent continuum approach [14,15] and the method whereby a number of representative channels are modelled [6]. The model developed here uses an equivalent continuum approach.

## GOVERNING EQUATIONS

The equations that predict the thermofluid dynamics and chemistry that occur in catalysts have been established for sometime. If an equivalent continuum approach is being used the general transport and conservation equations need to be modified slightly. The equations given below are essentially those described by Zygourakis [14]. They have been extended to include the behaviour of the exhaust gas outside the catalyst monolith and rearranged into the forms in which they were implemented within the CFD code.

For the fluid dynamics that occur in the inlet pipework, diffuser and outlet cone the Reynolds averaged Navier-Stokes equations are solved. Closure is provided by use of one of the standard turbulence models. The flow in the monolith substrate is assumed to be unidirectional and laminar with the cross sectional shape of each channel being taken as circular. Neglecting entrance effects the governing equation for such flow is give by the Hagen-Poiseuille equation,

$$\frac{\partial p}{\partial x} = -\frac{32\nu\rho u}{b^2} \qquad (1)$$

The temperature of the exhaust gas, $T_g$, is obtained by solving the conservation equation for the gas enthalpy,

$$\frac{\partial \rho_g h_g}{\partial t} + \nabla.\left(\rho_g U h_g\right) - \nabla.\left(\frac{k_g}{c_{pg}} \nabla h_g\right) = S1 \qquad (2)$$

The temperature is calculated using the expression,

$$h_g = c_{pg} T_g \qquad (3)$$

The source term S1 in EQ (2) is only active in the part of the calculation domain representing the catalyst. It is given by,

$$S1 = \frac{h a_v}{c_{pg}}\left(T_s c_{pg} - h_g\right) \qquad (4)$$

It represents the transfer of heat between substrate and exhaust gas.

The conservation equations for the chemical species in the exhaust gas are of the form,

$$\frac{\partial \rho_g C_{gi}}{\partial t} + \nabla.\left(\rho_g U C_{gi}\right) - \nabla.\left(\rho_g D_i \nabla C_{gi}\right) = S2 \qquad (5)$$

where $C_{gi}$ is the mole fraction of the species. Disassociation is assumed negligible. The source term S2 in EQ (5), like S1 in EQ (2), is only active in the catalyst. It is given by,

$$S2 = \rho_g K_{mi} a_v (C_{si} - C_{gi}) \qquad (6)$$

and similarly represents the transfer of chemical species between the substrate and exhaust gas. The concentrations of such species on the monolith surface, where the reactions take place, are governed by expressions of the form,

$$\frac{M_{Rg}}{10^3 \rho_g} a_c R_i = K_{mi} a_v \left(C_{gi} - C_{si}\right) \qquad (7)$$

Note that in common with accepted practise there is no transient term in EQ (7). This assumption is justified on the grounds that reaction rates occur so quickly they can be considered instantaneous. Thus species concentrations on the substrate at one time step have no influence on concentrations at the next time step.

The reaction rate expressions that have been used are those given by Oh and Cavendish [10]. To keep the computational effort of the present study to a minimum a single representative chemical reaction has been modelled. The reaction taken is the oxidation of CO, the relevant expressions being,

$$R_{CO} = k_1 C_{sCO} C_{sO_2} / T_g J_1 J_2 J_3 \qquad (8)$$

where,

$$J_1 = (1 + K_1 C_{sCO} + K_2 C_{sC_3H_6})^2 \qquad (8a)$$

$$J_2 = (1 + K_3 C^2_{sCO} C^2_{sC_3H_6}) \qquad (8b)$$

$$J_3 = (1 + K_4 C_{sNO})^{0.7} \qquad (8c)$$

$$k_1 = 6.699 \times 10^{13} \exp(-12556/T_s) \qquad (8d)$$

$$K_1 = 65.5 \exp(961/T_s) \qquad (8e)$$

$$K_2 = 2.08 \times 10^3 \exp(361/T_s) \qquad (8f)$$

$$K_3 = 3.98 \exp(11611/T_s) \qquad (8g)$$

$$K_4 = 4.79 \times 10^5 \exp(-3735/T_s) \qquad (8h)$$

The variable that links all the others together is the temperature of the substrate $T_s$. It is the only variable that can be transported between adjacent monolith channels. The equation governing its behaviour is essentially that of heat conduction in a solid. However, because an equivalent continuum approach is being used the orthotropic nature of the heat conduction in a monolith must be taken into consideration. Thus the governing equation becomes,

$$\rho_s \frac{\partial T_s}{\partial t} - \frac{k_s}{c_{ps}} \left\{ \frac{\partial^2 T_s}{\partial x^2} + \frac{G}{(1-\varepsilon)} \left( \frac{\partial^2 T_s}{\partial y^2} + \frac{\partial^2 T_s}{\partial z^2} \right) \right\} = S3 + S4 \qquad (9)$$

Note that x is the flow direction of the gas, whereas y and z are the Cartesian directions perpendicular to the flow. G is defined as $k_{eff}/k_s$, where $k_{eff}$ is the effective thermal conductivity of the composite of exhaust gas and substrate in the direction of y and z. The two source terms S3 and S4 are given by,

$$S3 = \frac{h a_v}{(1-\varepsilon) c_{ps}} \left(T_g - T_s\right) \qquad (10)$$

$$S4 = \frac{a_c R_i \Delta H_i}{(1-\varepsilon) c_{ps}} \qquad (11)$$

S3 represents the transfer of heat between the substrate and gas. S4 represents the heat released through the chemical reactions.

Several auxiliary relationships are used within the model. The density of the gas is obtained from the ideal gas law. Where it is not assumed constant the viscosity of the gas is given by,

$$\nu = (6.542 \times 10^{-11} T_g^{\,2}) + (6.108 \times 10^{-8} T_g) - 0.89 \times 10^{-5} \qquad (12)$$

The heat and mass transfer coefficients, h and $K_{mi}$, are calculated from Nusselt and Sherwood numbers respectively. For simplicity both are assumed constant throughout the monolith.

The boundary conditions used for the above equations vary from case to case. Because a general purpose CFD code is being used a large number of options are available.

## EQUATION IMPLEMENTATION

PHOENICS is a finite volume CFD code that provides solutions to differential equations of the general form,

$$\frac{\partial \rho \phi}{\partial t} + \nabla.(\rho U \phi) - \nabla.(\rho \Gamma \nabla \phi) = S \qquad (13)$$

where $\phi$ stands for any conserved property. $\Gamma$ is the kinematic diffusivity and S any source terms. In its standard set up the code is able to solve up to 50 different $\phi$'s, however 15 are reserved for special variables such as velocity, pressure and enthalpy. Each $\phi$ can be associated with either one of two phases. By default the conservation equation for any variable will consists of a transient term, a convection term and a diffusion term. To allow flexibility a facility is provided for cancelling any of these terms. Source terms can be set externally by the user.

The fluid dynamics equations are implemented as they would normally be within PHOENICS. The only

region of the calculation domain where they require special treatment is within the monolith. To model unidirectional laminar flow a computational grid should be used that consists of a series of parallel 'computational channels' (see Figure 1), their direction being the same as the actual monolith channels. Preventing momentum transfer between computational channels isolates them from their neighbours. Thus each channel obtains a uniform velocity profile with no viscous friction at its walls, a situation that produces a zero pressure drop. The user can then adjust the pressure drop caused by the flow to be a function of whatever is desired by introducing momentum sinks. For the present model the appropriate momentum sink is given by EQ (1). It is set as a source term in the relevant momentum equation. To simulate the reduced flow volume caused by the presence of the monolith the streamwise porosities of the cells are adjusted to the appropriate value. With the exception of the monolith the boundary conditions for the velocity field are those normally used for turbulent flow simulations.

Like the velocity components and the pressure, the enthalpy and the species concentrations in the gas are standard variables. Again both require special treatments within the monolith. Transport by convection and diffusion perpendicular to the flow direction must be prevented and the source terms S1 and S2 must be set. The temperature of the gas is automatically calculated using EQ (3) when the appropriate option is selected.

The expression for the species concentrations on the substrate, EQ (7), is different from other conservation equations in that it has no diffusion, convection or transient terms. Solutions however can still be obtained using the standard features of PHOENICS. If one of the $\phi$'s is used as one of the species concentrations and has all three of the built in terms switched off a source-term-only equation is left, for which solutions are still found. Thus the two sides of EQ (7) are introduced as source terms that are only active in the monolith. Consequently no solutions are given for the $C_{si}$'s anywhere else in the calculation domain.

The one remaining variable that needs to be solved is $T_s$. Inspection of EQ (9) reveals that it consists of a diffusion term, a transient term and two source terms. Thus a similar approach to that adopted for the $C_{si}$'s can be used. One of the unused $\phi$'s is taken as $T_s$, which then has its convection term switched off. Unfortunately because of the way the code handles the solution of any variable a special treatment is required for the transient term and the diffusivity. In both cases the density of the phase to which the variable is associated forms an integral part of their discretized mathematical representation. In the present model this density is taken as the gas density. Obviously the density that should appear in these terms is the density of the substrate, which is a constant. If the gas density could be taken as constant a simple cross multiplication could be implemented, however it varies with space and time. The only way found of overcoming its presence in the transient term was to cancel the term completely and introduce a hand built discretized transient term as an additional source term. The presence of the gas density in the substrate diffusivity can be cancelled with some FORTRAN code in the open access part of PHOENICS. The orthotropic nature of the thermal conductivity of EQ (9) is implemented by adjusting the diffusivity of the cell faces in the appropriate directions.

The method of solving EQ (9) outlined above may appear complex. An alternative that was considered was to make $T_s$ a variable that belongs to a second phase which has a different density to the first phase. However difficulties were experienced obtaining realistic results when simply trying to model the fluid dynamics of the catalyst system. In addition, significantly more computational effort is required when solving for two phase flow.

Solutions to EQ (9) are only required in the part of the calculation domain representing the monolith. The method adopted means that by default solutions are provided for the whole calculation domain. The computational cells in the monolith can be isolated from the rest of the domain by setting an adiabatic boundary at its front and rear faces. However computational effort is still expended on calculating values for $T_s$ where they are not required; an unavoidable drawback of the method.

## MODEL VALIDATION

For any computational model to be of use it must give realistic results. The best way of checking the accuracy of results is to compare them with experimental data. Unfortunately only limited experimental data is available at present. An initial assessment of a model's performance can still be made however by comparing its results with published results from other models. A suitable model is the one presented by Chen, Oh et al. [15], which not only gives extensive results but also includes details of the material properties and boundary conditions used.

The simulations that were run for comparison with Chen, Oh et al.'s work were for an axisymmetric catalyst assembly with (i) a uniform velocity profile and (ii) a non-uniform velocity profile. Both cases had adiabatic external catalyst walls. The non-uniform velocity profile was generated by using a conical inlet diffuser of length 0.1m and wall angle 14.8°. For computational economy the outlet cone was omitted. The profile predicted by the model (Figure 2) is typical of the profiles measured experimentally on catalysts with no outlet cone. Although the monolith could have been modelled on its own with a velocity profile entered as an inlet condition, an inlet diffuser has been used to demonstrate that

converged solutions can be obtained for a complete system. Unfortunately reference [15] does not present an adiabatic case similar to case (ii) above. There is however a similar non-adiabatic case with a more pronounced parabolic velocity profile. Comparison was made with the results from this case.

A number of other differences exist between the two models. Because the details from reference [15] are incomplete some further assumptions had to be made. In particular the exhaust gas properties were taken as those of air, with the gas density being calculated from the ideal gas equation and the viscosity taken as constant. To avoid overcomplication a number of refinements that were included in [15] have been omitted, such as making $c_{ps}$ a function of temperature. These differences are considered to be of secondary importance. One major difference between the models was that the present model only simulates the oxidation of CO. To try and simulate the effects of including other species conversions a multiplication factor, f, was used on the enthalpy of reaction. It was found that a value of between 1.2 and 1.3 gave reasonable results.

Table 1

CATALYST PARAMETERS FOR CASES (i) AND (ii)

| | | |
|---|---|---|
| Monolith Dimensions: | | |
| | L | 152.0 mm |
| | r | 46.48 mm |
| | b | 1.017 mm |
| | $\varepsilon$ | 0.6408 |
| | $a_v$ | 1981 $m^2/m^3$ |
| | $a_c$ | $537.9 \times 10^4$ $m^2Pt/m^3$ |
| Material Properties: | | |
| | $\rho_s$ | 1537 $kg/m^3$ |
| | $c_{ps}$ | 1000 J/kgK |
| | $k_s$ | 1.476 W/m K |
| | G | 0.1795 |
| | $M_{Rg}$ | 29 kg/kmol |
| | $c_{pg}$ | 1089 J/kg K |
| | $Pr_g$ | 0.7 |
| | $D_{CO}$ | $1.332 \times 10^{-4}$ $m^2/s$ |
| | $K_{mCO}$ | 0.4793 m/s |
| Inlet Conditions: | | |
| | $C_{gCO}$ | 0.02 mol/mol |
| | $C_{gNO}$ | $5.0 \times 10^{-4}$ mol/mol |
| | $C_{gC_3H_6}$ | $4.5 \times 10^{-4}$ mol/mol |
| | $C_{gO_2}$ | 0.05 mol/mol |
| | $\dot{m}$ case (i) | 18 g/s |
| | case (ii) | 25 g/s |

A listing of the material properties and inlet conditions is included in Table 1. Throughout the simulations the standard k-e turbulence model was used to close the fluid dynamics equations. The initial conditions were $T_s$ = 300 K, with a step increase in exhaust temperature to 650 K. The initial values for the velocity field where taken from a non-reacting steady state simulation. The Nusselt and Sherwood numbers where both taken to be equal to 3.66. Both cases were run with f values of 1.2 and 1.3. The change in conversion efficiency is illustrated in Figure 3. The evolution of the substrate temperature with time is shown in Figures 4 to 7. The data presented has been selected such that direct comparison can be made with the results from [15].

From the conversion data it can be seen that light-off, the point at which appreciable conversion is achieved, occurs between 3 and 7 seconds. Virtually all the conversion takes place in the first 2 to 3 cm of the monolith, and although not shown light-off commences here too. The differences in the monolith temperature distributions between the two cases illustrates the influence of a non-uniform velocity profile. For case (ii) a peak temperature occurs in the centre of the monolith, for case (i) the temperatures are uniform across the flow. Comparison with the results presented in reference [15] is very favourable.

Both the above simulations are based on conditions that are somewhat different from those that might be expected to occur in a real catalyst. Step increases in gas temperatures are not experienced, ramp or exponential temperature rises being more realistic. In addition it is generally accepted that Nusselt and Sherwood numbers vary along a monolith channel. There is also evidence [16] that the asymptotic values used for the Sherwood number are an order of magnitude too high. In an attempt to model more realistic catalyst light-off conditions a simulation was run that had a ramp increase in the gas inlet temperature from 400 K to 600 K in 100 seconds. A reduced mass transfer coefficient of 0.1 m/s was also used (corresponding to a Sherwood number of 0.764). The mass flow rate was set at 35 g/s, $a_c$ at 28790 $m^2Pt/m^3$ and v calculated using EQ (12). Apart from these changes the simulation was the same as case (ii) with f = 1.2. Figures 8 to 11 present the evolution of $T_s$, $T_g$, pressure and $C_{gCO}$ with time.

From these results it can be seen that up to 60 seconds there is essentially no conversion of CO, which is why these $C_{gCO}$ contours have been omitted. In this period the predominant process is the transfer of heat from the gas to the monolith. Appreciable conversion only commences when the monolith temperatures reaches 600 K, at between 60 and 80 seconds. Light-off takes place in the front third of the monolith, the peak temperature occurring just behind the 'reaction front'. From 80 to 100 seconds the conversion process becomes

more concentrated towards the front of the monolith. The peak temperature however moves further to the back. In essence the gas temperatures mirror the behaviour of the monolith temperature. As the temperature of the gas increases its viscosity increases, resulting in an increased catalyst back pressure by a factor of 2.8. Although no direct comparison can be made with experimental data, the results from this simulation are qualitatively more realistic.

## CONCLUDING REMARKS

The aim of this paper was to demonstrate that a commercial CFD code could be used to model the important physical and chemical phenomena that occur in automotive catalysts. Although the model contains many simplifications and assumptions it has been demonstrated that it can predict the gross effects known to exist in automotive catalysts. Thus even in its present relatively crude state the model can be used to carry out a number of parametric studies. Further work is required to properly validate the model, which will be carried out by collecting experimental data and comparing it with predicted results.

A number of refinements can be made to the model. These include,

(i) the modelling of more than one reacting species,

(ii) improving the values of the heat and mass transfer coefficients by making them a function of the fluid properties and distance along the monolith channels,

(iii) the modelling of external heat loss and the thermal inertia effects of the catalyst matting and can. Point (iii) could be implemented using the conjugate heat transfer options within PHOENICS. The others require additional FORTRAN coding in the open access part of the code.

## NOMENCLATURE

$a_c$ - catalyst area per unit reactor volume, $m^2Pt/m^3$
$a_v$ - ratio of reactor surface to reactor volume, $m^2/m^3$
$b$ - hydraulic diameter of monolith channels, m
$c_{pg}$ - specific heat of exhaust gas, J/kg K
$c_{ps}$ - specific heat of monolith material, J/kg K
$C_{gi}$ - concentration of gas species i, mol/mol
$C_{si}$ - concentration of species i on monolith surface, mol/mol
$D_i$ - diffusivity of species i, $m^2/s$
$G$ - monolith orthotropic conductivity factor
$h$ - heat transfer coefficient, $W/m^2$ K
$\Delta H_i$ - heat of reaction of species i, J/mol
$h_g$ - enthalpy of exhaust gas, J/kg
$k_g$ - thermal conductivity of exhaust gas, W/m K
$k_s$ - thermal conductivity of monolith material, W/m K
$K_{mi}$ - mass transfer coefficient for species i, m/s
$L$ - length of monolith, m
$\dot{m}$ - exhaust mass flow rate, kg/s
$M_{Rg}$ - relative molecular mass of exhaust gas, kg/kmol
$p$ - pressure, $N/m^2$
$Pr_g$ - Prandtl number of exhaust gas, $c_{pg}\nu\rho_g/k_g$
$r$ - radius of monolith, m
$R_i$ - reaction rate of species i, $mol/m^2Pt$ s
$t$ - time, s
$T_g$ - temperature of exhaust gas, K
$T_s$ - temperature of monolith, K
$u$ - axial velocity in monolith, m/s
$U$ - velocity of exhaust gas, m/s
$x,y,z$ - co-ordinate axes
$\varepsilon$ - monolith porosity
$\nu$ - kinematic viscosity, $m^2/s$
$\rho_g$ - density of exhaust gas, $kg/m^3$
$\rho_s$ - density of monolith material, $kg/m^3$

## ACKNOWLEDGEMENTS

The authors wish to acknowledge the financial and technical support given by Jaguar Cars Ltd, and the financial support given by the Science and Engineering Research Council throughout the development of the model presented here.

## REFERENCES

1. Comfort, E.H. - Monolithic catalytic converter performance as a function of flow distribution - ASME Winter Annual Meeting, Paper No. 74-WA/HT-30, 1974.

2. Lemme, S.J. and Givens, W.R. - Flow through catalytic converters - An analytical and experimental treatment - SAE Paper 740243.

3. Howitt, J.S. and Sekella, T.C. - Flow effects in monolithic honeycomb automotive catalytic converters - SAE Paper 740244.

4. Lai, M.-C., Kim, J.-Y., Cheng, C.-Y., Li, P., Chui, G. and Pakko, J.D. - Three-dimensional simulations of automotive catalytic converter internal flow - SAE Paper 910200.

5. Bella, G., Rocco, V. and Maggiore, M. - A study of inlet flow distortion effects on automotive catalytic converters - ASME Journ. of Eng. for Gas Turbines and Power, Vol. 113, 1991, pp 419 - 426.

6. Will, N.S. and Bennett, C.J. - Flow maldistributions in automotive converter canisters and their effect on emission control - SAE Paper 922339.

7. Young, L.C. and Finlayson, B.A. - Mathematical models of the monolith catalytic converters: Part I. Development of model and application of orthogonal collocation - AIChE Journal, Vol. 22, 1976, pp 331 - 343.

8. Heck, R.H., Wei, J. and Katzer, J.R. - Mathematical modelling of monolith catalysts - AIChE Journal, Vol. 22, 1976, pp 477 - 484.

9. Lee, S.T. and Aris, R. - On the effects of radiative heat transfer in monoliths - Chem. Eng. Sci., Vol. 32, 1977, pp 827 - 837.

10. Oh, S.H. and Cavendish, J.C. - Transients of monolithic catalytic converters: response to step changes in freestream temperature as related to controlling automobile emissions - Ind. Eng. Chem. Production, Research and Development, Vol. 21, 1982, pp 29 - 37.

11. Ryan, M.J. Becker, E.R. and Zygourakis, K. - Light-off performance of catalytic converters: The effect of heat/mass transfer characteristics - SAE Paper 910610.

12. Fueyo, N. - 1-D simulation of a catalytic converter for cars - PHOENICS Demonstration Report PDR/CFDU/IC/35, CHAM Ltd, 1987.

13. Flytzani-Stephanopoulas, M., Voecks, G.E. and Charng, T. - Modelling of heat transfer in non-adiabatic monolith reactors and experimental comparisons of metal monoliths with packed beds - Chem. Eng. Sci., Vol. 41, 1988, pp 1203 - 1212.

14. Zygourakis, K. - Transient operation of monolith catalytic converters: A two-dimensional reactor model and the effects of radially nonuniform flow distributions - Chem. Eng. Sci., Vol. 44, 1989, pp 2075 - 2086.

15. Chen, D.K.S., Oh, S.H., Bissett, E.J. and Van Ostrom, D.L. - A three-dimensional model for the analysis of transient thermal and conversion characteristics of monolithic catalytic converters - SAE Paper 880282.

16. Ullah, U., Waldram, S.P., Bennett, C.J. and Truex, T. - Monolithic reactors: Mass transfer measurements under reacting conditions - Chem. Eng. Sci., Vol. 47, 1992, pp 2413 - 2418.

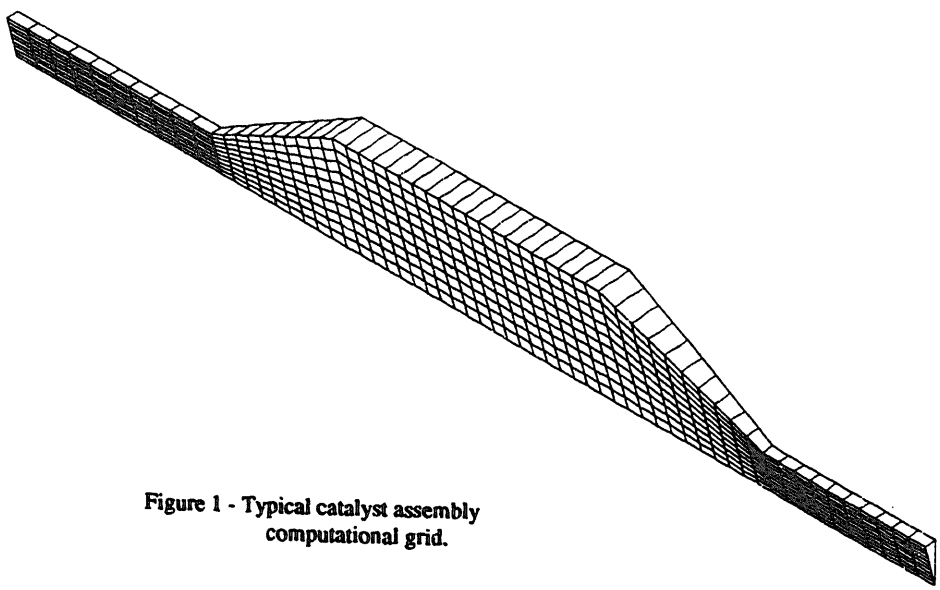

Figure 1 - Typical catalyst assembly computational grid.

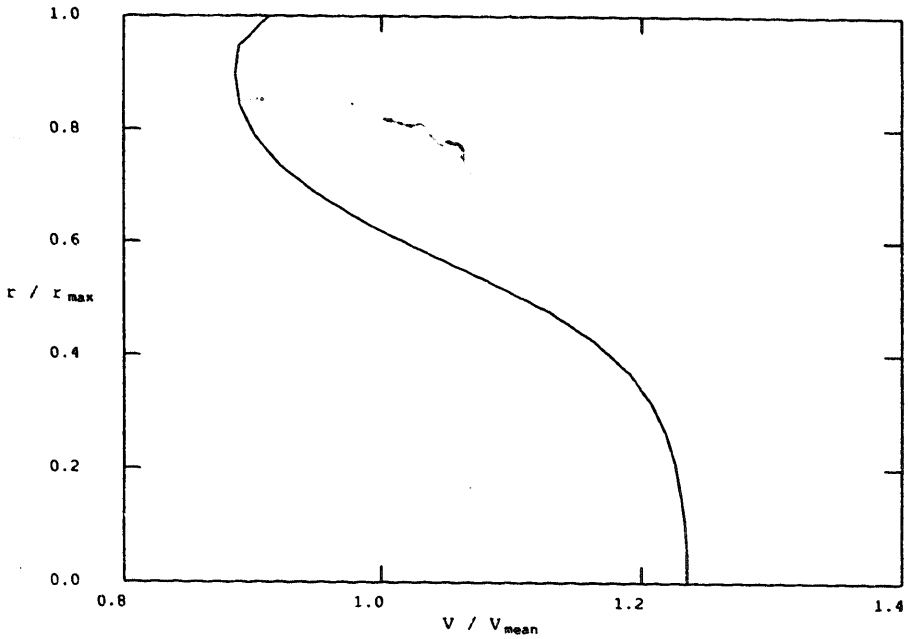


Figure 2 - Initial monolith inlet velocity profile for cases (i) and (ii).

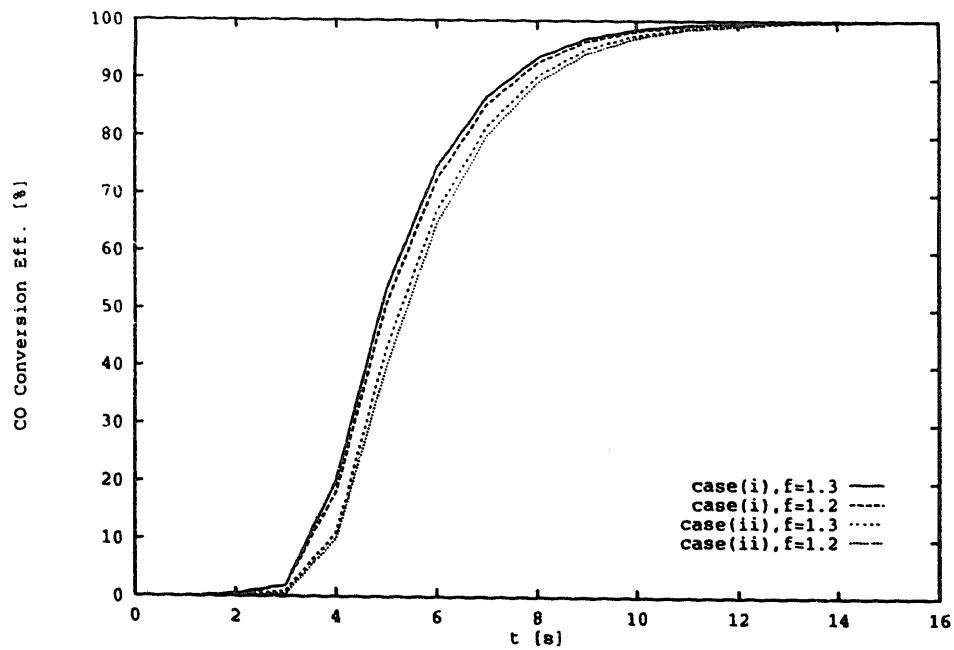


Figure 3 - CO conversion efficiency for cases (i) and (ii).

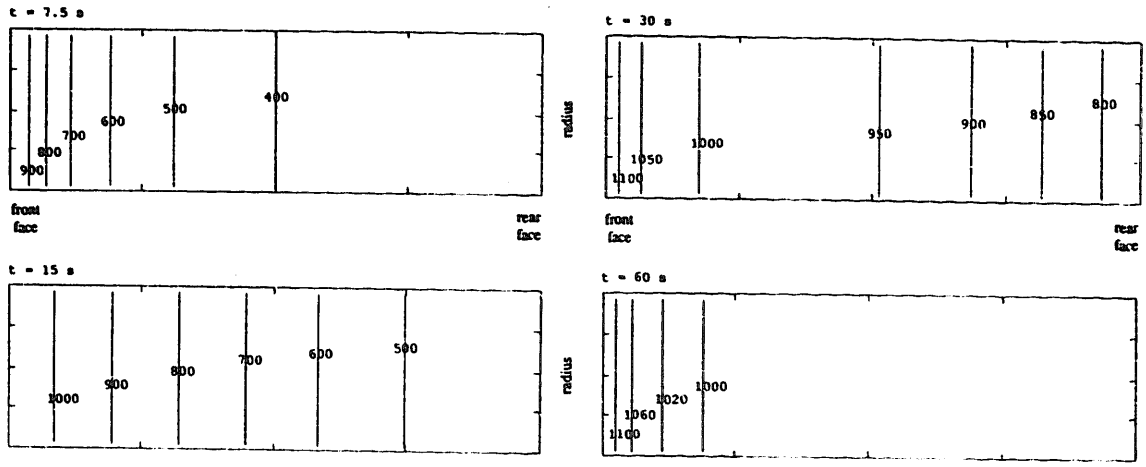


Figure 4 - Evolution of monolith temperature (in K) for case (i), F = 1.3.

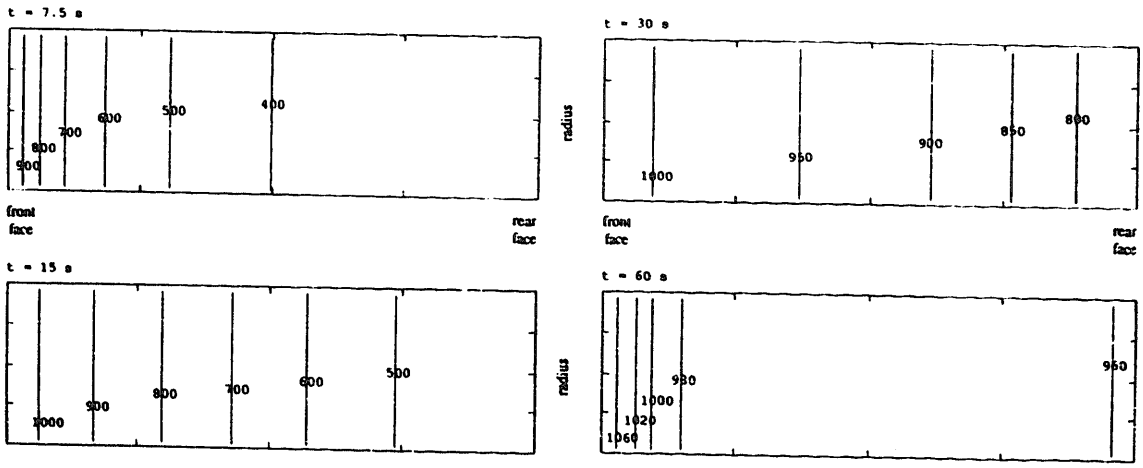


Figure 5 - Evolution of monolith temperature (in K) for case (i), F = 1.2.

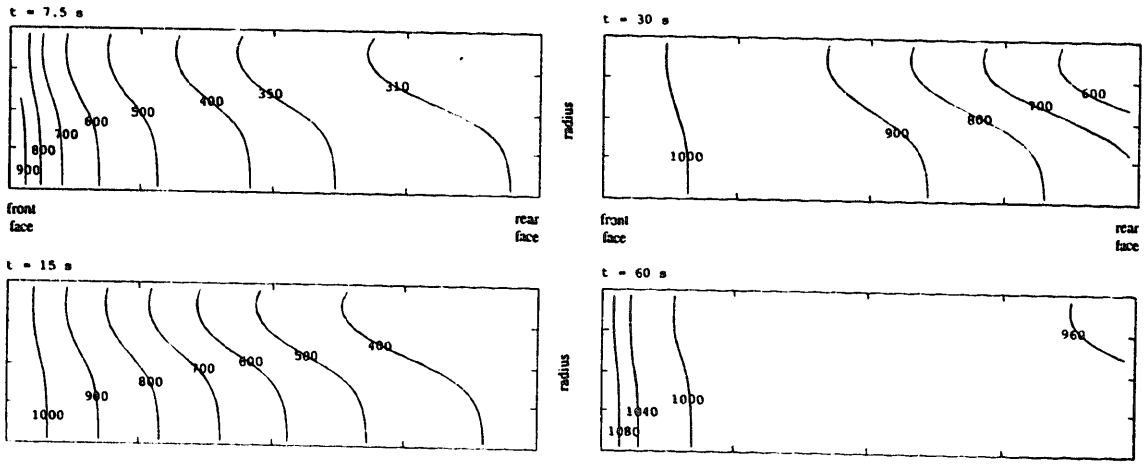


Figure 6 - Evolution of monolith temperature (in K) for case (ii), F = 1.3.

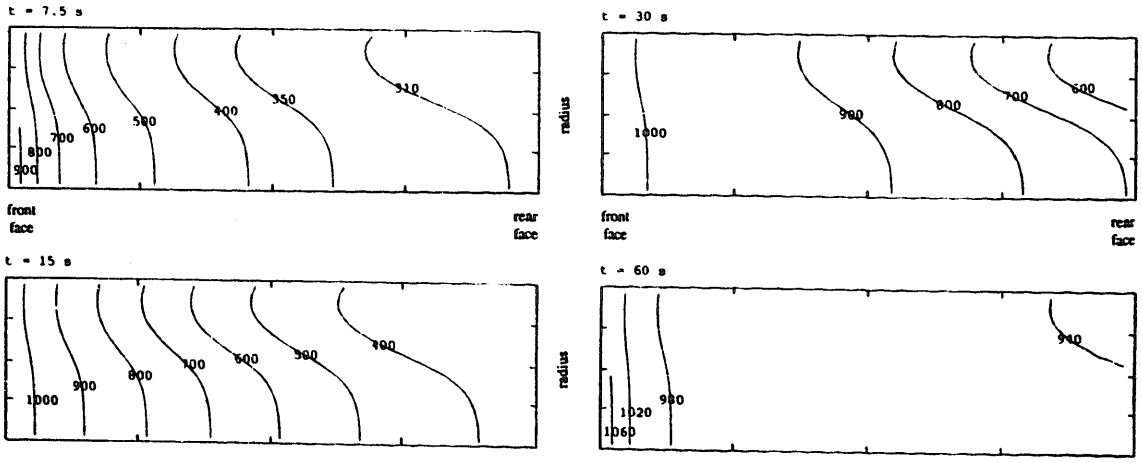


Figure 7 - Evolution of monolith temperature (in K) for case (ii), F = 1.2.

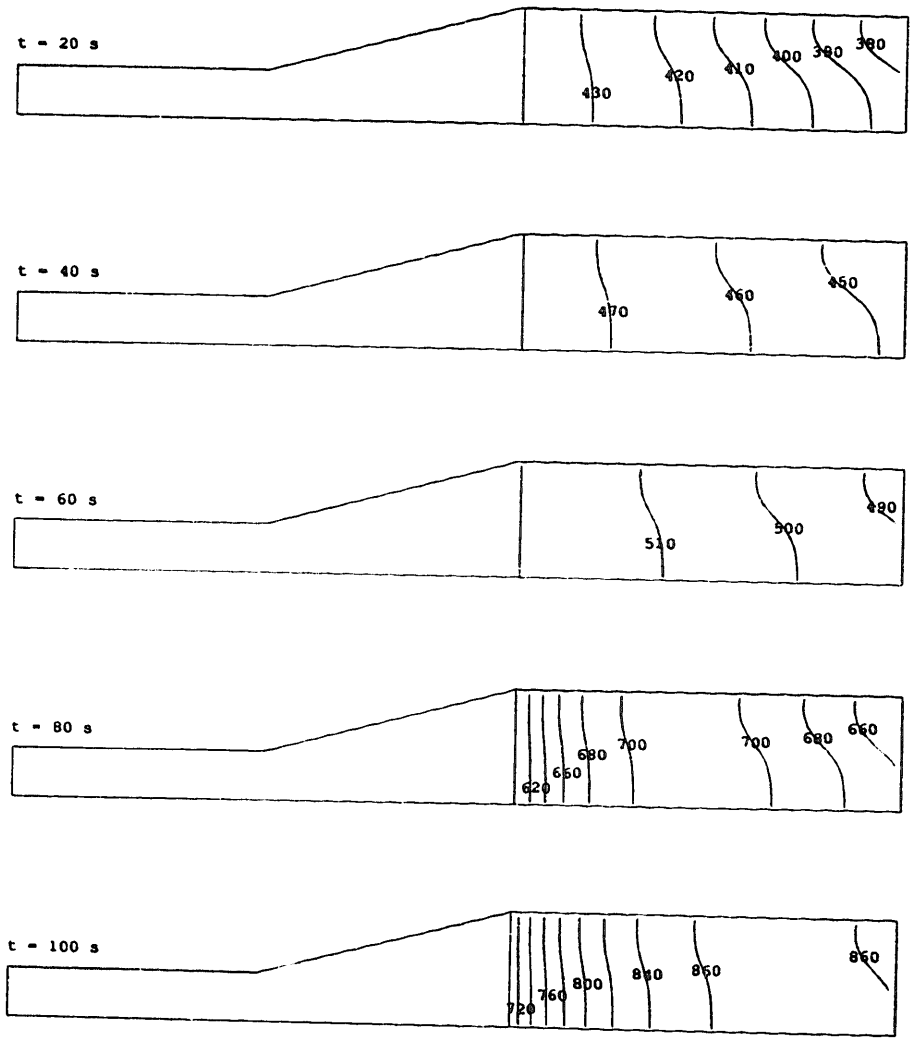


Figure 8 - Evolution of monolith temperature (in K) for ramp increase in $T_g$ case.

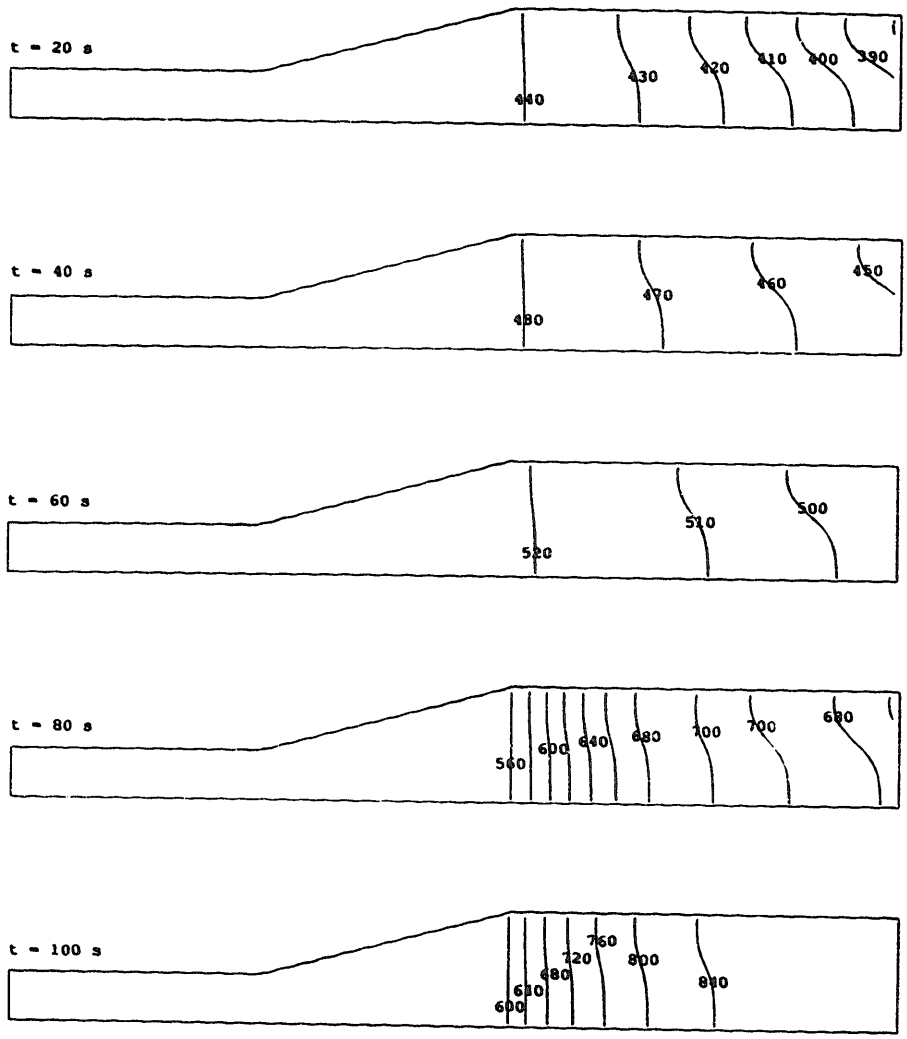


Figure 9 - Evolution of gas temperature (in K) for ramp increase in $T_g$ case.

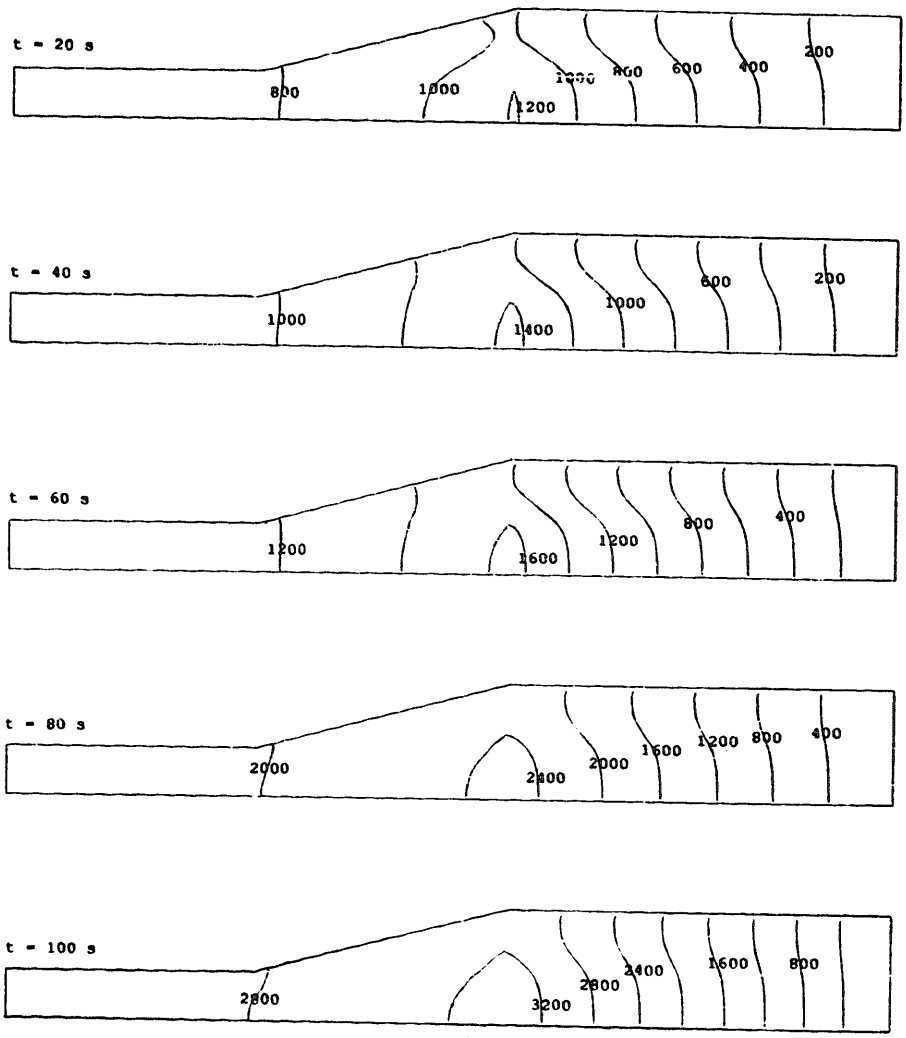


Figure 10 - Evolution of pressure (in $N/m^2$) for ramp increase in $T_g$ case.

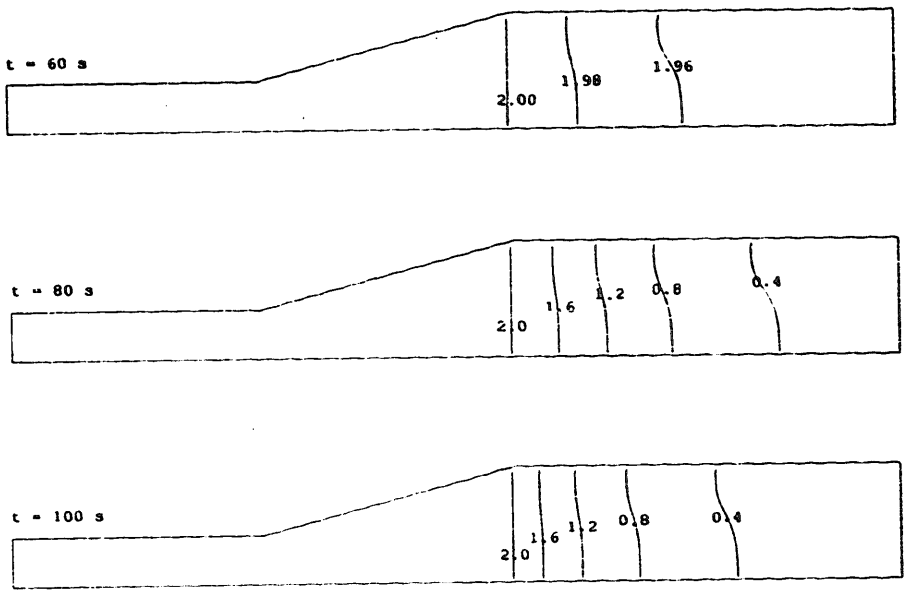


Figure 11 - Evolution of CO conversion (in % mol/mol) for ramp increase in $T_s$ case.